CAPTURED POWDER DAMPING IN ADDITIVE MANUFACTURING

Tony Schmitz[1,2], Emma Betters[1,2], and Justin West[1,2]
[1]Mechanical, Aerospace, and Biomedical Engineering
University of Tennessee, Knoxville
Knoxville, TN 37996, USA
[2]Energy and Transportation Science Division
Oak Ridge National Laboratory
Oak Ridge, TN 37830, USA

INTRODUCTION[1]

Additive manufacturing has been embraced as a disruptive technology for new production capabilities and strategies across multiple industries. Examples of its value include reduced part count in assemblies, maintenance and repair, and innovative structural designs [1]. Metal additive can be generally categorized by the feed material: powder or wire. Powder-based technologies include powder feed and powder bed. The layered melting or sintering of metal powder offers a unique opportunity for increased damping of printed components.

The dynamics of structures can be described by modal analysis, where the eigenvalues (or natural frequencies) and eigenvectors (or mode shapes) are used to define the vibration behavior. For any location on a structure, the frequency response function, or FRF, can be measured and the natural frequency, stiffness, and damping can be extracted for each mode [2]. Generally, it is desired to maximize the stiffness and damping to reduce the vibration magnitude due to external dynamic forces.

In this research, metal powder is intentionally retained within powder bed fusion structures to achieve increased damping. This internal, captured powder serves as an energy dissipation mechanism during vibration of the surrounding solid body. This work builds on seminal research by Scott-Emuakpor et al. [3-7]. This group first used laser powder bed fusion to produce components that contain internal geometries packed with powder trapped during layer-by-layer powder spreading and fusion. The application domain is integrally bladed rotors, where the monolithic design does not offer the airfoil-to-disk frictional energy dissipation for assembled designs. They studied damping for high strain-long duration tests and evaluated the endurance, repeatability, and recovery of the damping provided by unfused powder pockets in beam geometries. This research also adds to the prior work on particle dampers, which dissipate external energy within a constrained particle bed through collisions between the particles and container walls and collisions, sliding friction, and rolling friction between the individual particles [8].

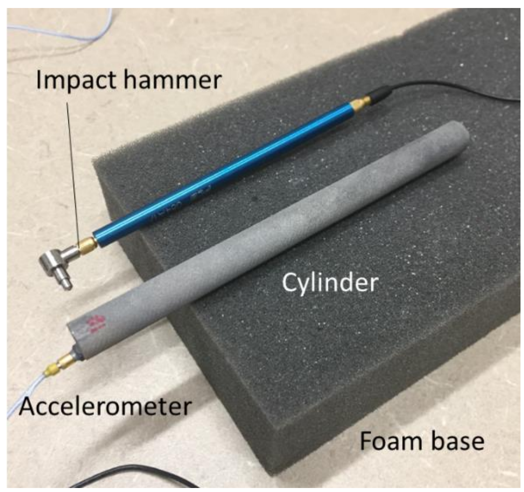

FIGURE 1: Impact testing setup for FRF measurement.

EXPERIMENTAL APPROACH

To demonstrate the potential for increased damping through captured powder, aluminum cylinders were designed and printed in a powder bed Concept Laser M2. Ingots of an aluminum-based alloy were produced by Eck Industries and atomized and sieved to a 20-63 µm size distribution (spherical shape) by Connecticut Engineering Associates Corporation. The nominally 10.3 mm diameter by 129.5 mm long cylinders were printed in a vertical orientation and then separated from the horizontal build plate using wire EDM. Solid and hollow filled geometries with different internal diameters were selected.

Modal testing was carried out by placing the cylinders on a soft foam base. This approximated free-free boundary conditions and eliminated the complication associated with providing a repeatable fixed boundary condition for cantilever testing. Impact testing was completed using a small impact hammer (PCB model 086E80), low-mass accelerometer (PCB model 352C23), and MLI's MetalMax TXF software. The measurement setup is shown in Fig. 1.

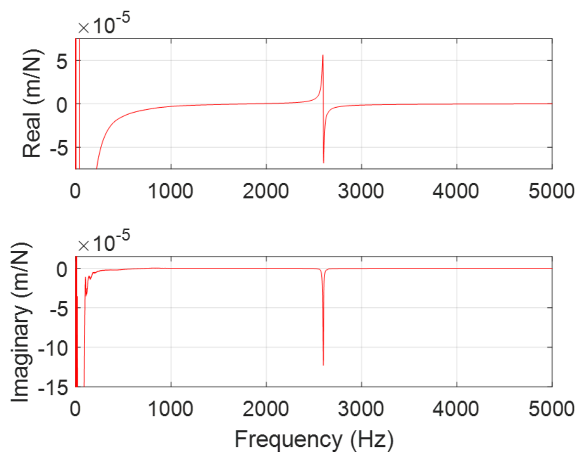

FIGURE 2: FRF for solid cross-section cylinder. (Top) Real part. (Bottom) Imaginary part.

The FRF for a 10.25 mm diameter, 129.4 mm long solid cross-section cylinder is displayed in Fig. 2. It is observed that the solid cylinder is lowly damped with a single bending mode at 2598 Hz. The large roll-off in the real part of the FRF at low frequencies is due to the free-free boundary conditions (i.e., rigid body modes). While the results are not included here for brevity, hollow cylinder (no powder fill) measurements were also completed and similar damping behavior to the solid cylinder was observed.

The FRF for a 10.29 mm outer diameter, 129.4 mm long hollow cross-section cylinder is displayed in Fig. 3, where the inner diameter is 4.9 mm (the design value was 5.1 mm). The same scale as Fig. 2 is shown; the bending mode is now at 2791 Hz. This inner diameter was estimated from a computed tomography (CT) scan of the cylinder since both ends were solid to contain the captured powder. Also, the powder fill for the internal volume was measured to be 97%. example results are presented in Fig. 4. From Fig. 3 it is observed that the captured powder increases the damping substantially based on the significant magnitude reduction (approximately an order of magnitude). The natural frequency also increases, primarily because the powder density is less than the solidified metal density.

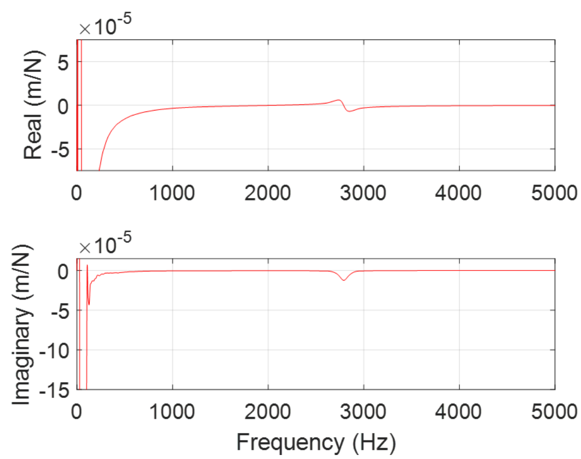

FIGURE 3: FRF for hollow cross-section cylinder with captured powder (4.9 mm inner diameter).

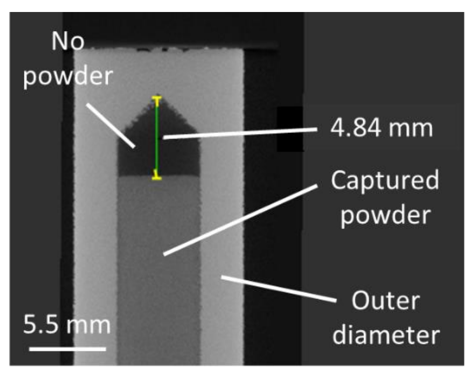

FIGURE 4: Example measurement result for 4.9 mm inner diameter cylinder. The density difference between the sintered outer diameter (light) and captured powder (dark) is identified by the image gray scale.

The FRF for a 10.30 mm outer diameter, 129.3 mm long hollow cross-section cylinder is displayed in Fig. 5, where the inner diameter is 9.0 mm (the design value was 9.1 mm) and the powder fill for the internal volume was measured to be 93%. The same scale as Fig. 2 is again shown; the bending mode is now at 2605 Hz. It is observed that the additional volume of captured powder due to the larger inner diameter further increases the damping. The natural frequency decreases due to the reduced wall thickness and associated stiffness.

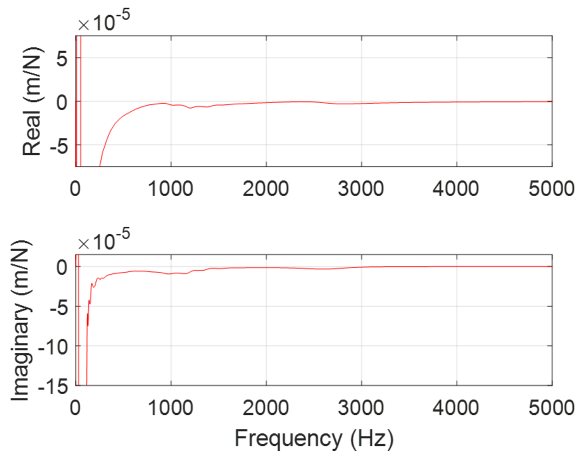

FIGURE 5: FRF for hollow cross-section cylinder with captured powder (9.0 mm inner diameter).

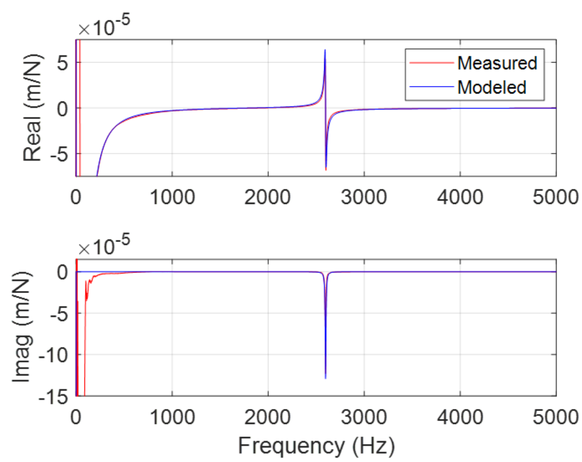

FIGURE 6: Measured and modeled FRF for solid cross-section cylinder.

MODELING

In order to extract damping values from the Fig. 2, 3, and 5 results, receptance coupling substructure analysis, or RCSA, was implemented to model the beams. In this approach, constant cross-sections are modeled using Timoshenko beam theory and then their receptances (or FRFs) are coupled to predict the assembly dynamics. Use of the Timoshenko beam model for the individual sections enabled structural damping to be incorporated as the complex modulus, $E' = E(1 + i\eta)$, where E is the elastic modulus and η is the dimensionless structural damping factor. The details of the RCSA procedure are provided in [2] and are not repeated here.

Initially, the 10.25 mm outer diameter, 129.4 mm long solid cross-section cylinder was modeled, where the density was determined from mass measurement and the cylinder dimensions, and the elastic modulus and damping factor were treated as fitting parameters. The modulus was used to match the measured natural frequency and the damping factor was used to match magnitude. The RCSA model prediction is compared to the measurement in Fig. 6. The free-free model parameters are provided in Table 1.

TABLE 1: RCSA model parameters for solid cross-section cylinder.

Model parameter	Value
Outer diameter (mm)	10.25
Length (mm)	129.4
Elastic modulus (GPa)	63.2
Density (kg/m^3)	2693.5
Damping factor (-)	0.004

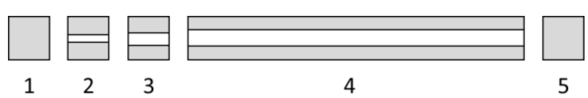

FIGURE 7: RCSA model for hollow cylinders. Five separate sections were rigidly coupled to predict the direct assembly receptance at the left end.

Next, the two hollow cylinders were modeled. The cross-sections are identified in Fig. 7 and the RCSA parameters are listed in Tables 2 (4.9 mm inner diameter) and 3 (9.0 mm inner diameter). Note that sections 2-4 were powder filled and the powder elastic modulus was assumed to be zero (no bending resistance). A comparison between the measured and modeled FRFs for the 4.9 mm inner diameter cylinder is displayed in Fig. 8.

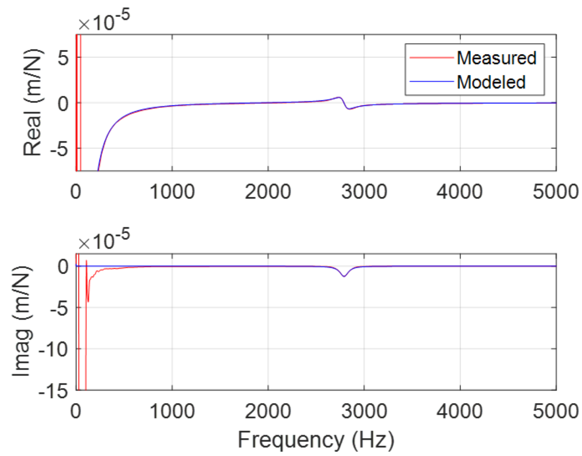

FIGURE 8: Measured and modeled FRF for hollow cross-section cylinder with captured powder (4.9 mm inner diameter).

TABLE 2: RCSA model parameters for hollow cross-section cylinder (4.9 mm inner diameter).

	Section				
Model para-meter	**1**	**2**	**3**	**4**	**5**
Outer dia. (mm)	10.29	10.29	10.29	10.29	10.29
Inner dia. (mm)	0	1.225	3.675	4.9	0
Length (mm)	3.2	1.35	1.35	118.9	4.55
Outer modul. (GPa)	69.55	69.55	69.55	69.55	69.55
Inner modul. (GPa)	69.55	0	0	0	69.55
Outer density (kg/m^3)	2670.3	2670.3	2670.3	2670.3	2670.3
Inner density (kg/m^3)	2670.3	1338.7	1338.7	1338.7	2670.3
Damping factor (-)	0.004	0.039	0.039	0.039	0.004

RESULTS AND DISCUSSION

Figures 2, 3, and 5 demonstrate the additional energy dissipation provided by the captured powder. Tables 1-3 list the structural damping factors for the three cylinders. To provide a visual comparison, Figs. 9 and 10 plot the damping factors as a function of internal diameter and cross-sectional area. Fitting functions are also included. For diameter, the fourth-order fit is given by Eq. 1, where d is the inner diameter. For area, the second-order fit is given by Eq. 2, where A is the inner cross-sectional area. Both support the trend that increased powder volume provides increased energy loss and structural damping.

$$\eta = 0.004 + 5 \times 10^{-5} d^4 \tag{1}$$

$$\eta = 0.004 + 8 \times 10^{-5} A^2 \tag{2}$$

TABLE 3: RCSA model parameters for hollow cross-section cylinder (9.0 mm inner diameter).

	Section				
Model para-meter	**1**	**2**	**3**	**4**	**5**
Outer dia. (mm)	10.3	10.3	10.3	10.3	10.3
Inner dia. (mm)	0	2.25	6.75	9.0	0
Length (mm)	1.3	2.15	2.15	120.9	2.8
Outer modul. (GPa)	69	69	69	69	69
Inner modul. (GPa)	69	0	0	0	69
Outer density (kg/m^3)	2670.3	2670.3	2670.3	2670.3	2670.3
Inner density (kg/m^3)	2670.3	1366.8	1366.8	1366.8	2670.3
Damping factor (-)	0.004	0.33	0.33	0.33	0.004

CONCLUSIONS

This paper reported measurements and models for the increased damping provided by retention of metal powder within additively manufactured structures. Solid and hollow aluminum cylinders were fabricated in a powder bed Concept Laser M2 printer where the internal, captured powder in the hollow cylinders provided increased energy dissipation when acted on by external forces.

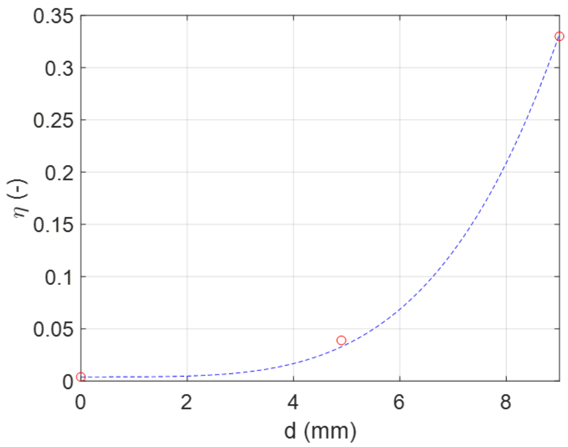

FIGURE 9: Damping factor data (circles) and fit (dashed line) versus inner diameter.

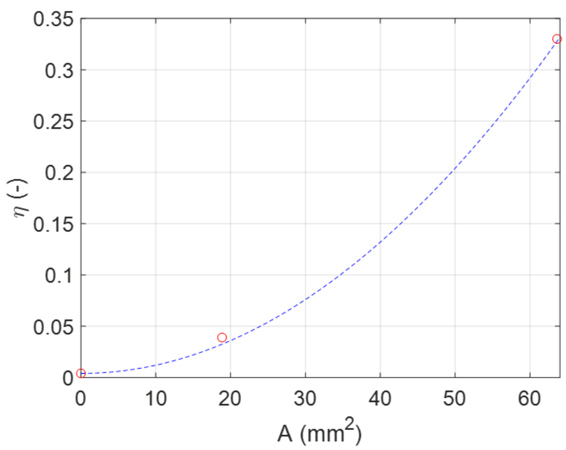

FIGURE 10: Damping factor data and fit versus inner cross-sectional area.

Free-free boundary condition impact testing was competed to compare the frequency response functions for three cylinder geometries: one solid cross-section and two hollow cross-sections with 4.9 mm and 9.0 mm inner diameters. It was observed that the frequency response function magnitude decreased with larger powder volumes, which indicated increased damping. The damping increase was quantified using a structural damping model. Timoshenko beam models of the cylinders' constant cross-sections were defined and rigidly joined using receptance coupling substructure analysis to predict the assembly dynamics. The dimensionless damping factor was considered a fitting parameter so its variation with cross-sectional geometry could be determined. It was observed that the damping factor increased with the fourth power of inner diameter and second power of inner cross-sectional area.

ACKNOWLEDGEMENTS

This research was supported by the DOE Office of Energy Efficiency and Renewable Energy (EERE), Energy and Transportation Science Division, and used resources at the Manufacturing Demonstration Facility, a DOE-EERE User Facility at Oak Ridge National Laboratory. The authors gratefully acknowledge Kevin Sisco, Alex Plotkowski, and Ryan Dehoff, ORNL, for the cylinder printing and Paul Brackman, Zeiss, for the computed tomography scans.

REFERENCES

[1] Frazier, W.E., 2014. Metal Additive Manufacturing: A Review. Journal of Materials Engineering and Performance, 23(6), pp.1917-1928.

[2] Schmitz, T.L. and Smith, K.S., 2011. Mechanical Vibrations: Modeling and Measurement. Springer Science & Business Media.

[3] Scott-Emuakpor, O., George, T., Runyon, B., Holycross, C., Langley, B., Sheridan, L., O'Hara, R., Johnson, P. and Beck, J., 2018, June. Investigating Damping Performance of Laser Powder Bed Fused Components with Unique Internal Structures. In ASME Turbo Expo 2018: Turbomachinery Technical Conference and Exposition. American Society of Mechanical Engineers Digital Collection.

[4] Scott-Emuakpor, O.E., George, T., Beck, J., Runyon, B.D., O'Hara, R., Holycross, C. and Sheridan, L., 2019. Inherent Damping Sustainability Study on Additively Manufactured Nickel-Based Alloys for Critical Part. In AIAA Scitech 2019 Forum (p. 0410).

[5] Scott-Emuakpor, O., George, T., Runyon, B., Sheridan, L., Holycross, C. and O'Hara, R., 2019, June. Assessing Manufacturing Repeatability of Inherently Damped Nickel Alloy Components via Forced-Response Testing. In Turbo Expo: Power for Land, Sea, and Air (Vol. 58677, p. V006T24A010). American Society of Mechanical Engineers.

[6] Scott-Emuakpor, O., George, T., Runyon, B., Langley, B., Sheridan, L., Holycross, C., O'Hara, R. and Johnson, P., 2019. Forced-Response Verification of the Inherent

Damping in Additive Manufactured Specimens. In Mechanics of Additive and Advanced Manufacturing, Volume 8 (pp. 81-86). Springer, Cham.

[7] Scott-Emuakpor, O.E., Beck, J., Runyon, B. and George, T., 2020. Multi-Factor Model for Improving the Design of Damping in Additively Manufactured Components. In AIAA Scitech 2020 Forum (p. 1631).

[8] Gagnon, L., Morandini, M. and Ghiringhelli, G.L., 2019. A Review of Particle Damping Modeling and Testing. Journal of Sound and Vibration, p.114865.